Photoluminescence from $Si_{1-x}Ge_x$ alloy nanocrystals

Shinji Takeoka and Kimiaki Toshikiyo
Division of Mathematical and Material Science, The Graduate School of Science and Technology, Kobe University, Rokkodai, Nada, Kobe 657-8501, Japan

Minoru Fujii,* Shinji Hayashi, and Keiichi Yamamoto
Department of Electrical and Electronics Engineering, Faculty of Engineering, Kobe University, Rokkodai, Nada, Kobe 657-8501, Japan
(Received 27 December 1999)

Photoluminescence (PL) from $Si_{1-x}Ge_x$ alloy nanocrystals (nc-$Si_{1-x}Ge_x$) as small as 4–5 nm in diameter was studied as a function of the Ge content. The nc-$Si_{1-x}Ge_x$ samples were fabricated by the cosputtering of Si, Ge, and SiO_2 and postannealing at 1100°C. High-resolution transmission electron microscopy, electron diffraction, and Raman spectroscopy clearly showed the growth of spherical $Si_{1-x}Ge_x$ nanocrystals in SiO_2 matrices. The PL spectra of nc-$Si_{1-x}Ge_x$ were found to be very sensitive to the Ge content. A low-energy shift of the PL peak from the widened band gap of Si nanocrystals to that of Ge nanocrystals with increasing Ge content was clearly observed.

I. INTRODUCTION

In recent years, great effort has been devoted to investigating the photoluminescence (PL) properties of nanometer size Si and Ge crystals.[1–3] In particular, many studies have been performed for Si nanocrystals (nc-Si) because of their potential application to Si-based optoelectronic devices. A high-energy shift of the PL peak and an increase in the PL intensity with decreasing size have commonly been observed in the near-infrared (NIR) to red regions.[4–7] Recently, Polisski *et al.* reported a continuous shift of the PL peak from the bulk band gap to the red region.[8] These strong size dependences indicate that the PL in the NIR to red regions originates from recombination of free excitons confined in nc-Si. In contrast to nc-Si, clear size dependence had not been observed until recently for Ge nanocrystals (nc-Ge). Many authors claimed that nc-Ge samples exhibit a PL peak around 2.2 eV independent of the size.[9–12] Size-dependent PL from nc-Ge has now been observed by some of the present authors.[13] We demonstrated that the PL peak shifts from 0.9 to 1.5 eV with decreasing size from 5 to 1 nm, and the PL intensity increases by about two orders of magnitude. From the observed size dependence, we concluded that the PL arises from the recombination of free excitons confined in nc-Ge.

As for pure nc-Si and nc-Ge, in the case of nanometer size $Si_{1-x}Ge_x$ alloy crystals (nc-$Si_{1-x}Ge_x$), the quantum confinement of carriers is expected to play an important role in determining the optical response. Since the energy band structure of bulk $Si_{1-x}Ge_x$ alloy crystals strongly depends on x,[14,15] that of nc-$Si_{1-x}Ge_x$ should depend on x as well as the particle size. It is expected that the band gap energy of nc-$Si_{1-x}Ge_x$ will change continuously from the widened band gap of nc-Si to that of nc-Ge with increasing x. Furthermore, shortening of the lifetime of the excitons by the alloying is theoretically predicted,[16] and an increase in the PL efficiency with the Ge content is expected.

Recently, Tang *et al.* fabricated $Si_{1-x}Ge_x$ quantum dots on ordered mesoporous silica.[17] They reported a low-energy shift of the PL peak with increasing Ge content. Lebib *et al.* observed visible PL from porous $Si_{1-x}Ge_x$ and demonstrated that the PL lifetime of porous $Si_{1-x}Ge_x$ is shorter than that of porous Si.[18] However, these authors did not succeed in evaluating the size of the particles. It is thus still unclear how the band structure of nc-$Si_{1-x}Ge_x$ changes with the size and x. Systematic studies controlling the size and x are highly desirable to understand the optical properties of nc-$Si_{1-x}Ge_x$.

In this work, we have succeeded in preparing nc-$Si_{1-x}Ge_x$ samples with 4–5 nm diameter and with a Ge content (x) of 0 to 0.31 by applying the cosputtering method. The samples were studied by high-resolution transmission electron microscopy (HRTEM), electron diffraction, Raman spectroscopy, and PL spectroscopy. We demonstrate that the PL peak energy of nc-$Si_{1-x}Ge_x$ samples as small as 4–5 nm in diameter shifts from that of nc-Si to that of nc-Ge with increasing Ge content. We also discuss the PL mechanism of pure nc-Si from the observed x and size dependences of the PL spectra.

II. EXPERIMENTAL PROCEDURE

$Si_{1-x}Ge_x$ alloy nanocrystals embedded in SiO_2 matrices were prepared by a rf cosputtering method. Si, Ge, and SiO_2 sputtering targets were simultaneously sputtered in Ar gas of 0.3 Pa (background pressure of 5×10^{-6} Pa) using a multitarget sputtering apparatus. The deposition rates can be controlled separately by changing the rf power and the distance between the substrate and the target. In this work, those of Si and SiO_2 were fixed and that of Ge was varied to control the Ge content in the films. The substrates were (100)-oriented Si wafers for Raman measurements and fused-quartz plates for PL measurements. The typical deposition rate was 10 nm/min, and the thickness of the films was about 300 nm. After the deposition, the films were annealed in N_2 gas at ambient pressure and 1100°C to grow nc-$Si_{1-x}Ge_x$ in SiO_2 matrices. The Ge content (x) was changed from 0 to 0.31. The values of x were determined by electron probe microanalysis (EPMA). For EPMA measurements, $Si_{1-x}Ge_x$

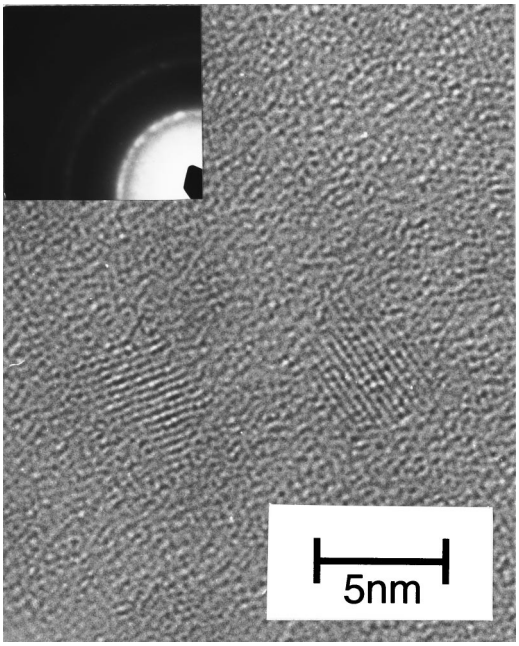

FIG. 1. Cross-sectional HRTEM image and electron diffraction pattern of a sample with $x=0.27$. The electron diffraction pattern demonstrates that the nanocrystals have the diamond structure.

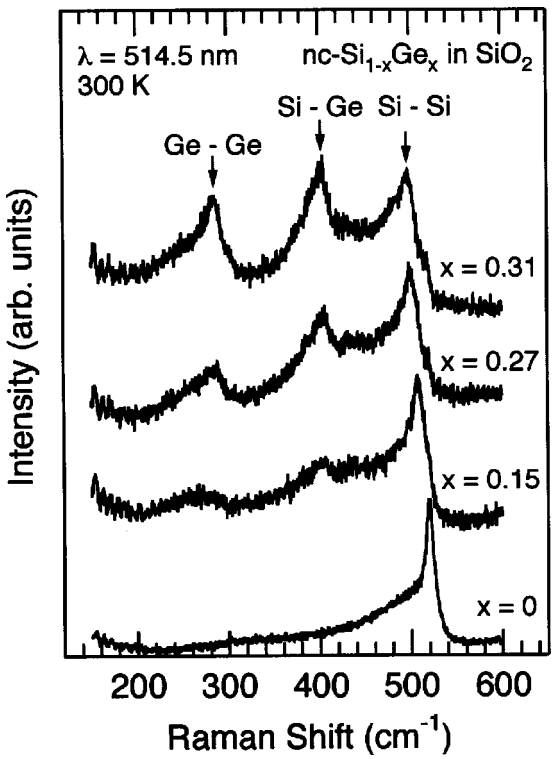

FIG. 2. Dependence of the Raman spectra of nc-$Si_{1-x}Ge_x$ on the Ge content.

alloy films were deposited on Cu plates by the cosputtering of Si and Ge to avoid the characteristic x-ray signals of Si atoms from the substrates and the SiO_2 matrices.

The Raman spectra were measured at room temperature. The excitation source was the 514.5 nm line of an Ar-ion laser. The Raman measurements were carried out in a $X[Y,Z]\overline{X}$ configuration, where the X, Y, and Z axes were parallel to the [100], [011], and $[01\overline{1}]$ axes of the Si substrate, respectively. In this configuration, the Raman signal at 520 cm^{-1} from the underlying Si substrate is so weak[19] that we can neglect the contribution of the substrate to the measured spectra.

The PL spectra were measured at room temperature using a single monochromator equipped with an InP/InGaAs photocathode near-infrared photomultiplier. The excitation source was the 457.9 nm line of an Ar-ion laser. The excitation power density was about 1 W/cm^2. The spectral response of the detection system was calibrated with the aid of the reference spectrum of a standard tungsten lamp. For the PL decay measurements, the 532.0 nm line of a Nd–yttrium aluminum garnet (YAG) laser was used as the excitation source. The pulse width and the repetition frequency were 5 ns and 20 Hz, respectively. The time resolution of the system was 80 ns.

After the optical measurements, the cross section of the samples was observed with a transmission electron microscope (TEM). The samples for the TEM observations were prepared by standard procedures including mechanical and Ar-ion thinning techniques.

III. RESULTS AND DISCUSSION

A. TEM observation and Raman study

Figure 1 shows a cross-sectional HRTEM image and the electron diffraction pattern of a sample with $x=0.27$. The HRTEM image clearly shows the growth of spherical nanocrystals in an amorphous SiO_2 matrix. Each nanocrystal is isolated from the others by SiO_2 barriers a few nanometers in thickness. The electron diffraction pattern demonstrates that the nanocrystals have the diamond structure. The lattice spacing of the first diffraction ring [(111) plane] is 0.321 nm. This value is between those of Si (0.314 nm) and Ge crystals (0.327 nm). The average diameter of the nanocrystals and the standard deviation determined from several HRTEM images were 4.6 and 1.1 nm, respectively. Cross-sectional HRTEM observation was performed for all the samples. We found that the average diameter of the nanocrystals slightly increases with increasing Ge content.

Figure 2 shows the Raman spectra of samples with various Ge contents. For the sample with $x=0$ (pure Si nanocrystals), a peak with a tail on the low-frequency side is observed around 520 cm^{-1}. This peak can be assigned to the TO phonon mode. The full width at half maximum of the peak is about 16 cm^{-1}, which is about five times larger than the bulk value (3.5 cm^{-1} at room temperature). The broadening of the peak and the appearance of the low-frequency tail are due to the relaxation of the momentum conservation rule.[20]

For the samples containing Ge atoms, three peaks are observed around 300, 400, and 500 cm^{-1}. In accordance with the spectrum of bulk $Si_{1-x}Ge_x$ alloy crystals,[21,22] these peaks are assigned to the Ge-Ge, Si-Ge, and Si-Si vibrations as indicated in the figure. As the Ge content increases, the intensity of the Ge-Ge and Si-Ge peaks increases, and for the sample with $x=0.31$, the intensity of the Si-Ge peak becomes comparable to that of the Si-Si peak. Moreover, the Si-Si peak shifts to lower frequencies, down to 497 cm^{-1}.

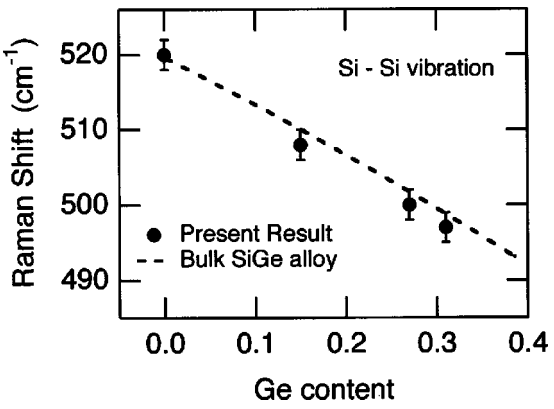

FIG. 3. Peak frequencies of the Si-Si vibration as a function of the Ge content. The error bars show the spectral resolution. The broken line is the data for bulk $Si_{1-x}Ge_x$ alloy crystals (from Ref. 21).

It is well known that, in bulk $Si_{1-x}Ge_x$ alloy crystals, the frequency of the Si-Si vibration is very sensitive to the Ge content.[21,22] In Fig. 3, we plot the peak frequencies of the Si-Si vibration as a function of the Ge content. The error bars show the spectral resolution. The broken line shows the data for bulk $Si_{1-x}Ge_x$ alloy crystals.[21] We can see that the present result agrees well with that for bulk $Si_{1-x}Ge_x$ alloy crystals. The relative intensity between the peaks also agrees well with that of bulk $Si_{1-x}Ge_x$ alloy crystals. The Raman spectra and the electron diffraction pattern shown in Fig. 1 indicate that the spherical nanocrystals observed in the HR-TEM images are indeed nc-$Si_{1-x}Ge_x$.

B. Photoluminescence study

The PL spectra of nc-$Si_{1-x}Ge_x$ with various Ge contents are shown in Fig. 4. The values of the average diameter of nc-$Si_{1-x}Ge_x$ determined from the HRTEM images are given on the left-hand side of each spectrum. The PL spectra are normalized at their maximum intensities and the scaling factors for the normalization are shown in the figure (a larger factor corresponds to a smaller PL intensity). For the sample with $x=0$ (pure Si nanocrystals), a PL peak is observed around 1.45 eV. Although not shown here, the PL peak shifted to higher energies and became intense with decreasing size.[6,7] The PL peak energy versus size relation was in good agreement with those reported for porous-Si and Si nanocrystals,[4,5] suggesting that the 1.45 eV PL originates from the radiative recombination of free excitons confined in nc-Si.

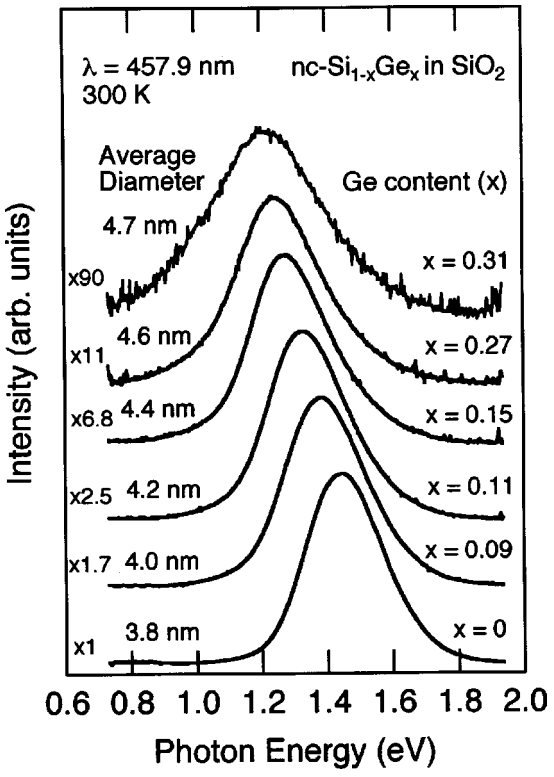

FIG. 4. PL spectra of nc-$Si_{1-x}Ge_x$ with various Ge contents.

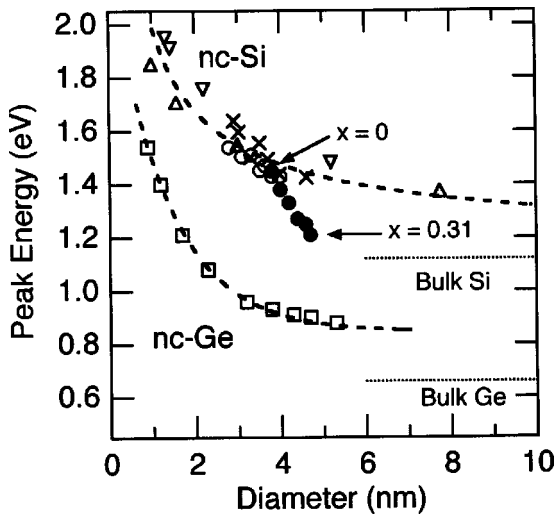

FIG. 5. PL peak energy versus average diameter of nanocrystals. Solid circles represent the present results (nc-$Si_{1-x}Ge_x$). The data on nc-Si and nc-Ge are taken from Ref. 4 (×), Ref. 5 (△,▽), Refs. 6 and 7 (○), and Ref. 13 (□). The broken curves are drawn to guide the eyes.

In Fig. 4, we can see that as the Ge content increases, the PL peak shifts to lower energies and reaches 1.21 eV for the sample with $x=0.31$. Although the size of nc-$Si_{1-x}Ge_x$ samples slightly increases with the Ge content, the observed shift is considered to be mainly caused by $Si_{1-x}Ge_x$ alloy formation. If the size of nc-Si increases from 3.8 to 4.7 nm, the shift of the PL peak is only 50 meV,[4–7] which is much smaller than the present shift ($\approx$240 meV).

In Fig. 5, the PL peak energies obtained from Fig. 4 are plotted as a function of the size (solid circle). For comparison purpose, the data for nc-Si (Refs. 4–7) and nc-Ge (Ref. 13) are also plotted. The broken curves are drawn to guide the eyes. We can see that the solid circles (present results) are located in between the two curves. With increasing Ge content, the solid circles deviate from the curve for nc-Si and approach that for nc-Ge. This figure clearly demonstrates that the PL energy of nc-$Si_{1-x}Ge_x$ is changed not only by the size of the nanocrystals but also by x.

As described above, recent experimental results suggest that the PL from nc-Si observed in the NIR to red regions arises from the radiative recombination of excitons confined in nc-Si.[4–8] The present results provide further evidence to support this model. If the PL originates from a localized state such as the oxygen related trap at Si/SiO_2 interfaces,[23–25] the PL energy should be nearly constant independent of the Ge

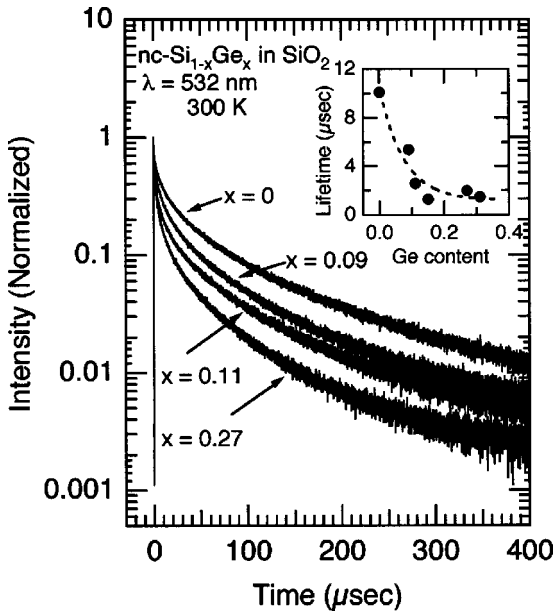

FIG. 6. PL decay curves monitored at the PL peak energies. The inset shows the dependence of the PL lifetime ($1/e$ time) on the Ge content.

content because the PL energy in that case will be governed by the local structures at the interfaces. We believe that the observed PL shift directly reflects the narrowing of the band gap of nc-Si by the $Si_{1-x}Ge_x$ alloying.

As shown in Fig. 4, the PL intensity decreases with increasing Ge content. The quenching of the PL intensity is considered to be caused by the following two factors. One is the slight increase in size. Since the size of nanocrystals studied in this work is close to the exciton Bohr radius of bulk Si crystals (4.9 nm),[1] the PL intensity is sensitive to the size. In our previous work, we reported that as the size of nc-Si increases from 3 to 4 nm, the PL intensity becomes about one order of magnitude weaker, and for nc-Si as large as 5 nm in diameter, the PL peak was too weak to be detectable.[6,7] The other factor quenching the PL is that the density of defects at the interface between nc-$Si_{1-x}Ge_x$ and surrounding SiO_2 matrices may increase with increasing Ge content. Schoisswohl *et al.* studied the density of defects for oxidized porous $Si_{0.8}Ge_{0.2}$ by using electron spin resonance measurements and reported that the density of the Ge P_b center is about 40 times larger than that of the Si P_b center.[26] This suggests that, in our samples, the density of defects increases with increasing Ge content. Since defects such as the P_b center act as nonradiative recombination centers at room temperature,[27] the PL intensity decreases with increasing Ge content.

Figure 6 shows the PL decay curves for various Ge contents. The decay curves are monitored at the PL peak energies. We can see that the lifetime for all the samples is on the order of a microsecond. The decay curve is multiexponential. We define the PL lifetime as the time at which the intensity becomes $1/e$ of the peak value. The inset of Fig. 6 shows the lifetime as a function of the Ge content. We found that the lifetime becomes shorter with increasing Ge content. The lifetime for $x=0$ is 10.1 μs, while that for $x=0.31$ is 1.5 μs. In the present study, the size of the nc-$Si_{1-x}Ge_x$ samples slightly increases with x. In general, the PL lifetime becomes longer with the size.[1–3] Therefore, if the size of nc-$Si_{1-x}Ge_x$ is fixed, the x dependence of the PL lifetime should be larger.

Two possible explanations are considered as the mechanism of the lifetime shortening. The first one is the increase in interface defects as described above and the resulting increase in the nonradiative recombination process via defects. The other mechanism is the increase in the oscillator strength of the excitons caused by the alloying.[16] At present, we cannot judge which mechanism is mainly responsible for the lifetime shortening.

Although we have succeeded in observing the size and x dependences of the PL energy and demonstrated that the band gap energy of nc-$Si_{1-x}Ge_x$ changes between that of nc-Si and that of nc-Ge depending on x, the detailed energy band structures and recombination kinetics of the excitons are still unclear. In particular, it is not clear whether or not the ratio of the no-phonon (quasidirect) to phonon-assisted (indirect) optical transitions depends on the size and x. Usually, the spatial confinement of electrons and holes in nc-Si and nc-Ge increases the uncertainty of the crystal momentum, and the no-phonon transition is expected to be partially allowed.[28,29] In the case of nc-Si, the ratio has been experimentally obtained by resonant PL measurements, and it was shown that the ratio increases with decreasing size.[28] It was also reported that in nc-Ge samples with 3–4 nm diameter the no-phonon transition becomes the dominant process, while in nc-Si with the same size the phonon-assisted transition is still the dominant process.[29] It is thus very plausible that the no-phonon transition plays a significant role in the recombination process for nc-$Si_{1-x}Ge_x$ with a small size and/or a high Ge content. Resonant PL studies of the present samples are now underway and the results will be published elsewhere.

IV. CONCLUSION

We have demonstrated that the PL energy of nc-$Si_{1-x}Ge_x$ can be tunable in a wide range from the NIR to red regions by combining two parameters, i.e., the size and x. The wide tunability is important for future applications of nc-$Si_{1-x}Ge_x$ as optoelectronic devices. The present results are also very important to understand the PL mechanism of nc-Si, because the results clearly demonstrate that the PL arises from the radiative recombination of excitons confined in nanocrystals and completely exclude the possibility that the PL arises from localized trap states.

ACKNOWLEDGMENTS

This work was supported by a Grant-in-Aid for Scientific Research from the Ministry of Education, Science, Sports and Culture, Japan, and a Grant for Research for the Future Program from the Japan Society for the Promotion of Science (JSPS-RFTF-96P-00305 and JSPS-RFTF-98P-01203). One of the authors (S.T.) would like to thank the Japan Society for the Promotion of Science for financial support.

*Author to whom correspondence should be addressed. Electronic mail: fujii@eedept.kobe-u.ac.jp

[1] A.G. Cullis, L.T. Canham, and P.D.J. Calcott, J. Appl. Phys. **82**, 909 (1997).
[2] *Light Emission in Silicon: From Physics to Devices*, edited by D. J. Lockwood (Academic Press, San Diego, 1998).
[3] D. Kovalev, H. Heckler, G. Polisski, and F. Koch, Phys. Status Solidi B **215**, 871 (1999).
[4] H. Takagi, H. Ogawa, Y. Yamazaki, A. Ishizaki, and T. Nakagiri, Appl. Phys. Lett. **56**, 2379 (1990).
[5] S. Schuppler, S.L. Friedman, M.A. Marcus, D.L. Adler, Y.-H. Xie, F.M. Ross, Y.J. Chabal, T.D. Harris, L.E. Brus, W.L. Brown, E.E. Chanban, P.F. Szajowski, S.B. Christman, and P.H. Citrin, Phys. Rev. B **52**, 4910 (1995).
[6] Y. Kanzawa, T. Kageyama, S. Takeoka, M. Fujii, S. Hayashi, and K. Yamamoto, Solid State Commun. **102**, 533 (1997).
[7] M. Fujii, S. Hayashi, and K. Yamamoto, in *Recent Research Development in Applied Physics*, edited by S. G. Pandalai (Transworld Research Network, Trivandrum, 1998), Vol. 1, p. 193.
[8] G. Polisski, H. Heckler, D. Kovalev, M. Schwartzkopff, and F. Koch, Appl. Phys. Lett. **73**, 1107 (1998).
[9] D.C. Paine, C. Caragianis, T.Y. Kim, Y. Shigesato, and T. Ishahara, Appl. Phys. Lett. **62**, 2842 (1993).
[10] M. Nogami and Y. Abe, Appl. Phys. Lett. **65**, 2545 (1994).
[11] Y. Maeda, Phys. Rev. B **51**, 1658 (1995).
[12] A.K. Dutta, Appl. Phys. Lett. **68**, 1189 (1996).
[13] S. Takeoka, M. Fujii, S. Hayashi, and K. Yamamoto, Phys. Rev. B **58**, 7921 (1998).
[14] G. Abstreiter, in *Light Emission in Silicon: From Physics to Devices* (Ref. 2), p. 37.
[15] J.C. Bean, in *Germanium Silicon: Physics and Materials*, edited by R. Hull and J.C. Bean (Academic Press, San Diego, 1999), p. 1.
[16] C. Delerue, G. Allan, and M. Lannoo, J. Lumin. **80**, 65 (1999).
[17] Y.S. Tang, S. Cai, G. Jin, J. Duan, K.L. Wang, H.M. Soyes, and B.S. Dunn, Appl. Phys. Lett. **71**, 2448 (1997).
[18] S. Lebib, H.J.V. Bardeleben, J. Cernogora, J.L. Fave, and J. Roussel, J. Lumin. **80**, 153 (1999).
[19] P.A. Temple and C.E. Hathaway, Phys. Rev. B **7**, 3685 (1973).
[20] I.H. Campbell and P.M. Fauchet, Solid State Commun. **58**, 739 (1986).
[21] M. A. Renucci, J. B. Renucci, and M. Cardona, in *Light Scattering in Solids*, edited by M. Balkanski (Flammarion, Paris, 1971), p. 326.
[22] M.I. Alonso and K. Winer, Phys. Rev. B **39**, 10 056 (1989).
[23] Y. Kanemitsu, T. Ogawa, K. Shiraishi, and K. Takeda, Phys. Rev. B **48**, 4883 (1993).
[24] S.M. Prokes and O.J. Glembocki, Phys. Rev. B **49**, 2238 (1994).
[25] M.V. Wolkin, J. Jorne, P.M. Fauchet, G. Allan, and C. Delerue, Phys. Rev. Lett. **82**, 197 (1999).
[26] M. Schoisswohl, J.L. Chamarro, H.J.V. Bardeleben, T. Morgenstern, E. Bugiel, W. Kissinger, and R.C. Andreu, Phys. Rev. B **52**, 11 898 (1995).
[27] M. Fujii, A. Mimura, S. Hayashi, and K. Yamamoto, Appl. Phys. Lett. **75**, 184 (1999).
[28] D. Kovalev, H. Heckler, M. Ben-Chorin, G. Polisski, M. Schwartzkopff, and F. Koch, Phys. Rev. Lett. **81**, 2803 (1998).
[29] S. Takeoka, M. Fujii, S. Hayashi, and K. Yamamoto, Appl. Phys. Lett. **74**, 1558 (1999).